Effects of carbon on the electrical and optical properties of InN, GaN, and AlN

J. L. Lyons,[*] A. Janotti, and C. G. Van de Walle

Materials Department, University of California, Santa Barbara, California 93106-5050, USA

(Received 5 November 2013; revised manuscript received 23 December 2013; published 16 January 2014)

Carbon is a common impurity in the group-III nitrides, often unintentionally incorporated during growth. Nevertheless, the properties of carbon impurities in the nitrides are still not fully understood. We investigate the impact of carbon impurities on the electrical and optical properties of GaN, AlN, and InN using density functional calculations based on a hybrid functional. We examine the stability of substitutional and interstitial configurations as a function of the Fermi-level position and chemical potentials. In all nitrides studied here, C_N acts as a deep acceptor and gives rise to deep, broad photoluminescence bands. Carbon on the cation site acts as a shallow donor in InN and GaN, but behaves as a DX center in AlN. A split interstitial is the most stable configuration for the C impurity in InN, where it acts as a double donor and likely contributes to n-type conductivity.

DOI: 10.1103/PhysRevB.89.035204 PACS number(s): 61.72.uj, 78.55.Cr, 71.55.Eq, 72.80.Ey

I. INTRODUCTION

The nitride semiconductors GaN, AlN, InN, and their alloys constitute the basic materials for green, blue, and ultraviolet light-emitting diodes and lasers [1], and are also used for high-frequency, high-power transistors [2]. Impurities (intentional or otherwise) can have a significant effect on the optical and electronic properties. Since nitride films are often grown using metal-organic precursors, carbon impurities are often incorporated in relatively high concentrations that may affect device operation. Indeed, significant concentrations of carbon have been detected in unintentionally doped AlN [3], in AlGaN alloys [4], and in InN [5].

Carbon is also deliberately incorporated into GaN to create semi-insulating buffer layers that improve the performance of AlGaN/GaN heterojunction field-effect transistors [6–8]. However, the mechanism whereby carbon makes GaN semi-insulating is still a subject of debate. For instance, it was suggested that C would incorporate on both N (as acceptor) and Ga (as donor) sites, leading to self-compensation [9]. Recently, we have found that carbon acts as a deep acceptor in GaN, and suggested that carbon substituting on the N site, by itself, can make GaN semi-insulating by pinning the Fermi level in the vicinity of its deep acceptor level [10]. The deep nature of the carbon acceptor can also account for the widely observed yellow luminescence in GaN [10–14] (though as discussed in Ref. [10], there is likely more than one source of yellow luminescence in GaN). Intriguingly, other studies have reported the observation of both blue and yellow luminescence in C-doped layers [13,15–17].

In AlN, carbon doping has been shown to give rise to a broad luminescence band, implying that the carbon impurity induces deep levels in the band gap [18–21]. In InN, the role of C has been less studied than in the other nitrides, but carbon concentrations have recently been found to correlate with n-type conductivity in molecular-beam epitaxy-grown InN [22]. Clearly, the impact of this impurity on the electrical and optical properties of GaN, AlN, and InN is still not completely established. Given its behavior as a deep level, carbon may play a role in radiative and nonradiative recombination, affecting device performance. A fuller understanding of its behavior and impact on electronic properties is necessary and timely.

The properties of C impurities in nitride semiconductors have previously been studied with first-principles methods based on density-functional theory (DFT), mainly using conventional functionals such as the local-density approximation (LDA) or generalized gradient approximation (GGA) [9,23–27]. Calculations using these techniques found that C acts as an acceptor when substituting on the N site, and as a donor on the cation site. In GaN and InN, acceptor ionization energies of 200–300 meV for C_N were reported, whereas C on the cation sites was found to act as a shallow donor [9,23–26]. In the case of AlN, it was reported that C_N acts as a shallow acceptor, and that C_{Al} acts as a deep donor [26,27].

A major shortcoming of LDA and GGA calculations is the large uncertainty in the position of defect levels (and hence also formation energies) due to the severe underestimation of the semiconductor band gap, as shown in Table I. Another significant issue is the inaccuracy of the position of the valence-band maximum (VBM) on an absolute energy scale in LDA and GGA, which also affects the value of formation energies [28,29]. The latter error is especially important to address when attempting to compare the stability of different forms of an impurity, especially when these defects have opposing charge states. As has been shown in previous work [10,19,28–33], using methods that address the band-gap error gives results that are qualitatively different than those obtained using LDA or GGA. This is particularly important for accurately describing deep, localized states, as demonstrated for C_N in GaN in our prior work [10] and recently also for C_N in AlN by Collazo *et al.* [19].

In this work we report results on the formation energies, ionization energies, and optical transition levels for the carbon impurity on substitutional and interstitial sites in GaN, AlN, and InN, expanding on previous work [10] in which we explored the behavior of substitutional carbon impurities in GaN. We consider C incorporation on cation, anion, and interstitial sites, and explore the possibility of off-site displacements (such as DX- and AX-like configurations). A DX center occurs when an impurity that is expected to act as a donor instead undergoes a large lattice relaxation and traps an electron to become a deep acceptor [34]. Analogously,

[*]jllyons@engineering.ucsb.edu

 ©2014 American Physical Society

TABLE I. Lattice parameters, band gap, and formation enthalpy for GaN, AlN, and InN calculated using DFT with the GGA and HSE functionals. Experimental values are taken from from Ref. [41].

Material	Property	GGA	HSE	Expt.[a]
	a (Å)	3.22	3.19	3.19
	c (Å)	5.22	5.17	5.19
GaN	E_g (eV)	1.57	3.51	3.50
	ΔH_f (eV)	–1.02	–1.33	–1.29
	a (Å)	3.12	3.10	3.11
	c (Å)	5.02	4.96	4.98
AlN	E_g (eV)	4.11	6.19	6.19
	ΔH_f (eV)	–2.87	–3.29	–3.30
	a (Å)	3.58	3.58	3.54
	c (Å)	5.80	5.77	5.70
InN	E_g (eV)	0.00	0.65	0.70
	ΔH_f (eV)	0.04	–0.20	–0.30

[a]Reference [41].

an AX center occurs when an impurity expected to be an acceptor undergoes a large lattice relaxation to trap a hole and become a deep donor [35]. For the cation sites, we find that C_{Ga} in GaN and C_{In} in InN behave as shallow donors; in AlN, we find a DX-like distortion associated with C_{Al}, and hence behavior as a deep level. C_N acts as a deep acceptor in the three nitrides and gives rise to broad sub-band-gap optical transitions. Furthermore, we find that C_N forms an AX center in AlN and GaN, i.e., it induces a donorlike $(+/0)$ level near the VBM. In InN, the $(+/0)$ transition level of C_N occurs just below the VBM. In all three materials, interstitial carbon prefers a split-interstitial configuration in which C_i and a host N atom share the same substitutional site. In AlN and GaN, we find that C_{cation} and C_i are much higher in energy than C_N. On the other hand, we predict C_i to be the most stable species in InN for Fermi-level positions within the band gap, acting as a double donor. Consequences of these behaviors for materials properties and device characteristics will be discussed.

II. METHODS

The calculations are based on the generalized Kohn-Sham scheme [36] with the hybrid functional of Heyd, Scuseria, and Ernzerhof (HSE) [37] as implemented in the VASP code [38,39]. In the HSE method, the exchange potential is divided in short-range and long-range parts with a screening length of 10 Å. In the short-range part, a fraction of nonlocal Hartree-Fock exchange potential is mixed with the GGA exchange potential of Perdew, Burke, and Ernzerhof (PBE) [40]. The long-range part and the correlation potential are described by the PBE functional. The mixing parameter for the Hartree-Fock potential is set to 0.25 for InN, 0.31 for GaN, and 0.33 for AlN, resulting in lattice parameters and band gaps that are in close agreement with the experimental values [41], as shown in Table I.

The interactions between the valence electrons and ionic cores are described through the use of projector-augmented wave potentials [42,43], with the Ga and In semicore d electrons treated as core electrons. Our tests have shown that explicitly including the semicore d electrons in the valence has a negligible effect on the formation energies and transition levels of the defects studied here. We perform defect calculations using a 96-atom supercell with periodic boundary conditions, a plane-wave basis set with a cutoff of 300 eV, and a $2 \times 2 \times 2$ Monkhorst-Pack k-point set.

The likelihood of incorporating an impurity in a crystal is determined by its formation energy. In the case of C on the Ga site in GaN, the formation energy is given by [44]

$$E^f\left(C_{Ga}^q\right) = E_{tot}\left(C_{Ga}^q\right) - E_{tot}(\text{GaN}) - \mu_C + \mu_{Ga} + q(E_F + \epsilon_v) + \Delta^q, \quad (1)$$

where $E_{tot}(C_{Ga}^q)$ is the total energy of the crystal containing one C_{Ga} in charge state q in the supercell, and E_{tot}(GaN) is the total energy of a perfect crystal in the same supercell. The Ga atom that is removed from the crystal is placed in a reservoir of energy μ_{Ga}, referenced to the total energy per atom of bulk Ga. The C atom that is added is taken from a reservoir with energy μ_C set to the energy per atom of bulk C in the diamond phase. In the case of charged defects the formation energy also depends on the Fermi level (E_F), i.e., the chemical potential of electrons, referenced to the bulk VBM, ϵ_v. Finally, Δ^q represents a correction for charged states due to the finite size of the supercell, applied following the procedure of Refs. [45] and [46].

Similarly, for the incorporation of C on the N site (C_N), the formation energy is given by

$$E^f\left(C_N^q\right) = E_{tot}\left(C_N^q\right) - E_{tot}(\text{GaN}) - \mu_C + \mu_N + q(E_F + \epsilon_v) + \Delta^q, \quad (2)$$

where $E_{tot}(C_N^q)$ is the total energy of the supercell containing one C_N in charge state q. The N atom that is removed from the crystal is placed in a reservoir of energy μ_N, referenced to the energy of an isolated N_2 molecule.

The transition level (or ionization energy) between charge states q and q' of an impurity is given by the Fermi-level position at which the formation energy of the impurity in charge state q is equal to that in charge state q'. In the case of C_N, the transition level $(0/-)$ is given by

$$(0/-) = E^f(C_N^-; E_F = 0) - E^f\left(C_N^0\right), \quad (3)$$

where $E^f(C_N^-; E_F = 0)$ is the formation energy when the Fermi level is at the VBM. Note that the transition level represents a thermal ionization energy and should not be confused with optical transition levels. The optical transitions occur on time scales much shorter than the time scales of lattice relaxations, and their energies can be extracted from configuration-coordinate diagrams, constructed following the procedure of Ref. [44].

III. RESULTS AND DISCUSSION

A. Bulk properties of GaN, AlN, and InN

The calculated lattice parameters, band gaps, and formation enthalpies of AlN, GaN, and InN are listed in Table I, along with the respective experimental values. For comparison, we also list the values calculated using the GGA functional [40]. We note that GGA slightly overestimates the lattice constants, while the HSE results are in better agreement with the

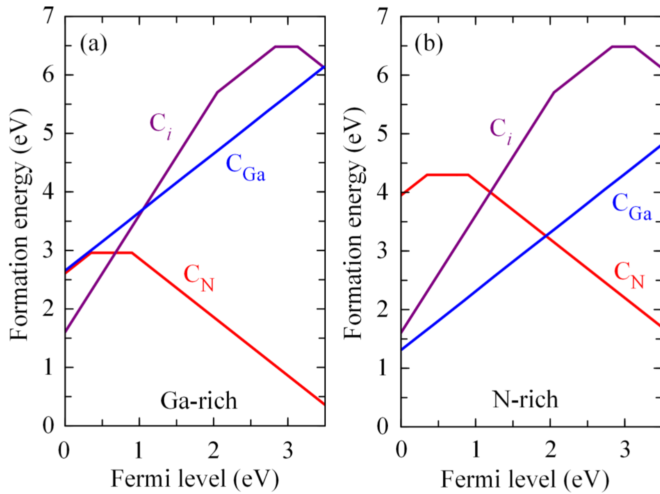

FIG. 1. (Color online) Formation energy versus Fermi level for substitutional C_{Ga}, C_N, and interstitial C_i configurations in GaN. (a) Ga-rich conditions. (b) N-rich conditions.

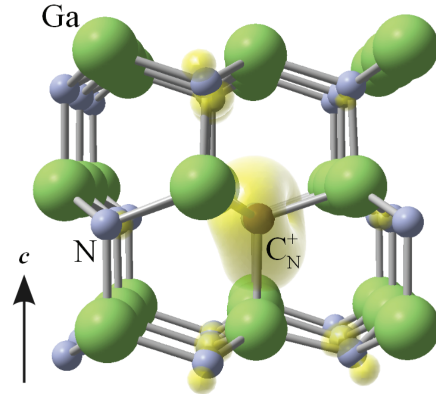

FIG. 2. (Color online) Structure and spin density associated with C_N^+ in GaN. The gap states for this center are composed of p-like carbon orbitals. The isosurface is set to 5% of the maximum.

experimental values. The formation enthalpies of the nitrides calculated using HSE are also in closer agreement with the experimental values. As expected, the GGA severely underestimates the band gap in all cases, and predicts InN to be a semimetal. The HSE corrects this problem.

B. Carbon impurities in GaN

1. C_{Ga} and C_i in GaN

We have previously reported on the properties of C_{Ga} and C_N in GaN, and the mechanism whereby the carbon acceptor C_N gives rise to yellow luminescence (YL) [10]. Here we also investigate the stability of C_i in GaN and the possibility of AX behavior of C_N. As shown in Fig. 1, our results for C_{Ga} are consistent with our previous study [10]. Consistent with other theoretical work [9,23], we find that C acts as a shallow donor when incorporating on the Ga site, and is stable in the positive charge state across the GaN band gap. The four nearest-neighbor N atoms relax inward by 26% of the N-Ga bond length for C_{Ga}^+. We have also explored possible DX-like configurations, in which either the neutral or negatively charged C_{Ga} is significantly displaced away from a nearest-neighbor nitrogen atom. While we do find metastable configurations for these charge states, they do not lead to transition levels within the calculated band gap of GaN, in agreement with previous work [9,26]. C_{Ga} is the lowest-energy configuration for the carbon impurity only for N-rich conditions and when the Fermi level is below midgap. As most as-grown, undoped samples of GaN are unintentionally n type, C_{Ga} will not be the most favored configuration for the carbon impurity when present as an unintentional impurity.

The formation energies of the most stable charge states of the carbon interstitial in GaN are also shown in Fig. 1. The lowest-energy configuration for C_i in GaN is the split-interstitial configuration (below we show an analogous configuration for the case of C_i in InN). C_i can assume charge states from 2+ to 2– in GaN. However, as Fig. 1 shows, C_i is the lowest-energy configuration only under extreme Ga-rich conditions and when E_F is near the VBM. Thus, under most conditions we predict that C_i will not be a relevant configuration for the carbon impurity.

2. Electronic properties of C_N in GaN

As previously reported [10], C_N is a deep acceptor with the (0/–) transition level at 0.90 eV above the VBM. Due to this very large ionization energy, it is clear that C_N will not give rise to p-type conductivity in GaN. Instead, incorporation of a large concentration of C_N will pin the Fermi level near its (0/–) transition level. This explains the experimental findings of carbon doping leading to semi-insulating layers [15], without the need to invoke precisely equal concentrations of donors and acceptors.

In the negative charge state (C_N^-), the four nearest-neighbor Ga atoms move inwards by 2% of the equilibrium N-Ga bond length. In the neutral charge state (C_N^0), an asymmetric distortion occurs whereby the C-Ga bond along the c axis becomes longer by 8%, while the other three C-Ga bonds become only 1% longer. Together with this distortion, the hole associated with C_N^0 occupies a highly localized orbital which is centered on the C impurity and is also oriented axially.

We find that C_N in GaN exhibits AX-like behavior, as shown in Fig. 2. For Fermi-level positions near the VBM, C_N traps a second hole, stabilizing the C_N^+ charge state. The (+/0) transition is 0.35 eV above the VBM. In this charge state, three C-Ga bonds are significantly elongated, by 10.8%, 8.7%, and 5.1%, compared to the equilibrium C-Ga bond. The other C-Ga bond is only 2% longer than the equilibrium C-Ga bond. The spin density of this charge state (an $S = 1$ center) is shown in Fig. 2, in which we see that the two unpaired electrons are localized on the C impurity, with a C $2p$ character.

3. Optical and trapping properties of C_N in GaN

We have also investigated the optical properties of C_N, going beyond the results presented in Ref. [10] by also including effects associated with the (+/0) transition level. In Fig. 3(a) we show the optical transitions associated with the (0/–) transition level. As previously reported, we find the $C_N^0 + e^- \rightarrow C_N^-$ process to give rise to yellow emission with a

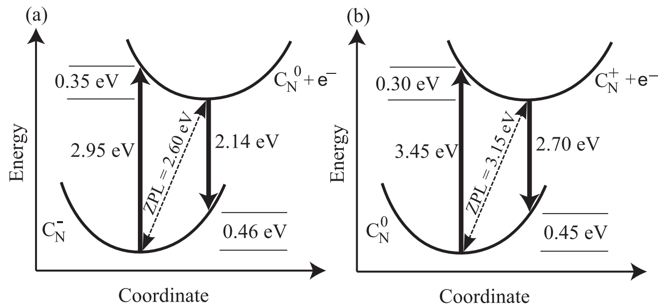

FIG. 3. Configuration-coordinate diagrams for the C_N impurity in GaN. (a) If electrons in the conduction band recombine with $C_{NN}^{0\,0}$, the emission associated with the $C_N^0 + e^- \rightarrow C_N^-$ transition is predicted to occur with a peak at 2.14 eV. (b) If electrons in the conduction band recombine with C_N^+, the emission associated with the $C_N^+ + e^- \rightarrow C_N^0$ transition is predicted to peak at 2.85 eV.

peak at 2.14 eV and a zero-phonon line (ZPL) at 2.60 eV. More recent calculations that include full vibronic coupling found that the calculated luminescence line shape of this transition agrees very well with the experimentally observed YL in carbon-containing samples [47].

The presence of the (+/0) transition level allows for the possibility of additional optical transitions associated with C_N. These transitions are shown in Fig. 3(b), in which we consider an exchange of an electron at the conduction-band minimum (CBM) with the (+/0) transition level. We predict the $C_N^+ + e^- \rightarrow C_N^0$ transition to give rise to blue emission peaking at 2.70 eV with a zero-phonon line at 3.15 eV, and a Franck-Condon shift of 0.45 eV. For the corresponding absorption process ($C_N^0 \rightarrow C_N^+ + e^-$), we predict a peak at 3.45 eV with a Frank-Condon shift of 0.30 eV. For these transitions, the configuration coordinate represents the outward relaxation of the nearest-neighbor Ga atoms.

These results demonstrate that the carbon acceptor in GaN can lead to yellow or blue emission, depending on the position of the Fermi level in the sample and the intensity of excitation during the photoluminescence (PL) experiment, since incident photons could ionize C_N^0 centers. In GaN with low concentrations of C (lightly or unintentionally doped), the samples will likely be n type due to background donors. C_N^- will then be the most stable charge state, and we expect the YL to be most prominent, occurring when optical excitation creates the C_N^0 charge state. Heavy C doping should lead to the appearance of blue luminescence (BL), as this will establish the Fermi level nearer to 0.9 eV above the VBM, stabilizing C_N^0. The BL process could then occur through optical excitation of C_N^0 to C_N^+. Such behavior has been observed in Refs. [13] and [17], in which the BL appeared in C-doped material after the concentration of C exceeded that of donor impurities. Photoluminescence experiments on C-doped GaN involving high excitation could also exhibit BL, even in nominally n-type samples, as a higher photon flux will be more likely to create not only C_N^0 but also C_N^+. Such behavior has been indeed observed in C-doped GaN in several studies [13,15,16]. Both BL and YL have been observed simultaneously in C-doped GaN [15], and high excitation [16] and heavy C doping [13,15,17] have been observed to increase the intensity of the BL.

Recently, the presence of YL has been correlated with "kink effects" (in which current-voltage curves show a sudden increase in drain current) in AlGaN/GaN high-electron-mobility transistors (HEMTs) [48]. Previously, kink effects in HEMTs had been attributed to impact ionization or field-dependent trapping of deep trap levels. Meneghesso *et al.* [48] reported that devices which exhibit kink effects also exhibit YL in their cathodoluminescence spectra, and that the kink effect can be modulated by illumination with sub-band-gap light, causing the authors to speculate that these effects are caused by a deep trap level. We note that the characteristics of this trap are consistent with C_N in GaN, raising the possibility that deep C_N acceptors influence HEMT performance. When incorporated unintentionally or as a buffer dopant, C_N gives rise to a deep acceptor level that can trap or emit carriers.

The carbon impurity has also been implicated in causing current collapse in AlGaN/GaN HEMTs and metal-semiconductor field-effect transistors (MESFETs) [49]. In Ref. [49], photoionization spectroscopy (PS) measurements showed that heavily C-doped GaN featured two deep traps in MESFET and HEMT structures. One of these traps ("Trap 2" in the study) correlated with carbon concentration. As noted by the authors, the PS spectra of the C-doped samples are very similar to the photoluminescence excitation data of C-doped GaN [11,12], as both feature an onset near 2.5 eV. This value also agrees well with the onset of absorption (at the energy of the ZPL) for C_N evident from our configuration-coordinate diagram in Fig. 3(a). These results highlight the important role that C-related traps play in current collapse in HEMTs. Because of the deep nature of C_N, E_F will be pinned near the (0/−) transition level of C-doped GaN. In such a situation, a large percentage of C_N will be present in the neutral charge state. These deep acceptors can then trap hot carriers from the conducting channel, which is thought to be the mechanism whereby current collapse occurs [49]. Deep trap levels near 0.9 eV that are likely related to C_N in GaN have recently been observed in deep level transient spectroscopy studies of C-doped GaN [50–52], further supporting the role of likelihood of C acting as a deep acceptor and carrier trap in GaN.

4. C_N complexes in GaN

Thus far we have focused on the role of isolated C_N in GaN. But, as C_N is a negatively charged acceptor in n-type GaN, it is also possible that the carbon acceptor could form complexes with donors. Recently, it has been suggested that O_N forms a complex with C_N in C-doped GaN [53]. However, in such a complex, the donor and acceptor are next-nearest neighbors, and would not be expected to be strongly bound. In fact, the calculated binding energy of such a complex is just 0.2 eV, indicating that only a small percentage of C_N acceptors will actually be bound in such complexes. Furthermore, the oxygen chemical potential (μ_O) in Ref. [53] was taken from the total energy of an O_2 molecule, and not limited by the formation of competing phases such as Ga_2O_3, resulting in formation energies for O_N and C_N-O_N complexes that are unrealistic.

Instead of O_N, we find that other donor impurities, such as interstitial hydrogen, are more likely to form stable complexes with C_N. Indeed, we find that H_i^+ forms a stable complex with C_N with a binding energy of 1.23 eV, with a C-H bond length

of 1.10 Å. The C_N-H_i complex has a (+/0) transition level of 0.25 eV above the VBM, and leads to optical transitions that are distinct from isolated C_N. We find that the emission associated with this center peaks at 2.76 eV, with a Franck-Condon shift of 0.49 eV and a zero-phonon line of 3.25 eV.

When hydrogen is present (as is the case during metal-organic chemical vapor deposition), the concentration of carbon on nitrogen sites will be enhanced, both due to the lowering of the formation energy of C_N when the Fermi level rises due to hydrogen interstitials acting as donors (Fig. 1), and due to the formation of C-H complexes. These C-H complexes are neutral for nearly all Fermi levels in GaN, with a formation energy of 1.36 eV. The effects of C-H complexes are similar to those reported for Mg-H complexes in GaN [54].

C_N^- could also form a complex with a C_i^{2+} donor. We find that these two species combine in the form of a split-interstitial center, with a binding energy of 2.62 eV. $(\text{C-C})_N^+$ is the lowest-energy charge state across the band gap of GaN, with a C-C bond length of 1.23 Å.

C. Carbon impurities in AlN

1. C_{Al} and C_i

In Fig. 5 we show the formation energies of C_{Al}, C_N, and C_i in AlN as a function of Fermi-level position. Unlike in GaN, C_{Al} is not a shallow donor in AlN: As shown in Fig. 5, C_{Al} can assume positive, neutral, and negative charge states in AlN, with both (+/0) and (0/−) levels occurring within the AlN band gap. We find the (+/0) transition level at 1.82 eV below the CBM, and the (0/−) transition level at 1.68 eV below the CBM. In the positive charge state, C_{Al}^+, the four N atoms relax inward by 17% of the N-Al bond length. In the negative charge state, C_{Al} assumes a DX-like configuration in which one nonaxial C-N bond is broken; the distance between this N atom and C atom increases by 64% of the Al-N bond length. The C atom moves past the plane of the other three nearest-neighbor Al atoms, and forms bonds that are 18% shorter than the bulk AlN bond length. The atomic configuration of C_{Al}^- is shown in Fig. 4. C_{Al}^0 is lower in energy than the positive or negative charge states only over a small range of Fermi levels,

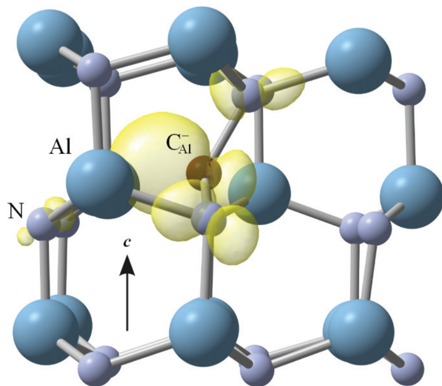

FIG. 4. (Color online) Structure and charge density associated with the gap state of C_{Al}^- in AlN. In this configuration the carbon atom is strongly displaced away from a planar N nearest neighbor, and this C-N bond is completely broken. The isosurface is set to 5% of the maximum.

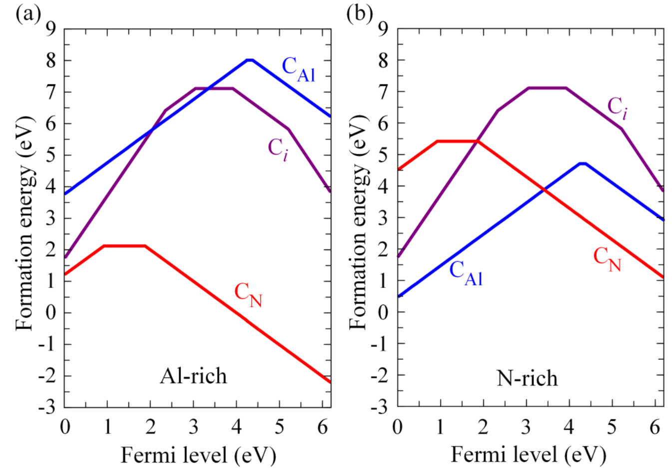

FIG. 5. (Color online) Formation energy versus Fermi-level position for C_{Al}, C_N, and C_i in AlN. (a) Al-rich conditions; (b) N-rich conditions.

and has a DX-like configuration similar to C_{Al}^-. As shown in Fig. 5, the C_{Al} species is the lowest-energy configuration only for Fermi levels in the lower part of the band gap, and under N-rich conditions.

Also shown in Fig. 5 are the formation energies of the charge states of the carbon interstitial in AlN. As in GaN, C_i can assume charge states from 2+ to 2− in AlN. However, as Fig. 5 shows, C_i is never the lowest-energy form of the C impurity in AlN, regardless of the position of E_F or of the chemical potential conditions. Thus, in equilibrium, C_i will not be a relevant configuration for carbon in AlN.

2. Electronic properties of C_N in AlN

Next we address the properties of the carbon acceptor in AlN. As shown in Fig. 5, the behavior of the C_N impurity in AlN is analogous to its behavior in GaN. It can exist in three charge states: C_N^+, C_N^0, and C_N^-. The (+/0) transition level is located 1.07 eV above the VBM and the (0/−) transition is 1.88 eV above the VBM, both of which are deeper than in GaN. The local lattice relaxations around C_N in each of its charge states are qualitatively similar to those in GaN. The nearest-neighbor Al atoms move outward by less than 1% for C_N^-. For C_N^0, the carbon is displaced slightly along the c axis, and the distance between C and its axial neighbor increases by 7% of the bulk bond length, while the planar Al-C bond lengths increase by 4%. For C_N^+ we find that the C atom is displaced off-site along the c axis by 5% of the N-Al equilibrium bond length, the axial Al-C bond is increased by 13%, one planar Al-C bond is increased by 10%, and the other two planar bond lengths increase by 5%.

3. Optical properties of C_N in AlN

We determined the optical transitions associated with C_N in AlN by constructing the configuration-coordinate diagrams shown in Fig. 6. Assuming that C_N^- is the ground-state configuration, the calculated absorption peak associated with the $C_N^- \rightarrow C_N^0$ transition occurs at 4.83 eV, with an emission peak at $(C_N^0 \rightarrow C_N^-)$ at 3.69 eV, and a zero-phonon line of 4.32 eV, as shown in Fig. 6(a).

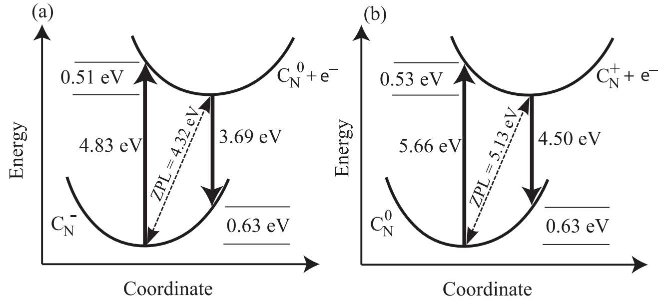

FIG. 6. Configuration-coordinate diagrams for the C_N impurity in AlN. (a) Assuming that C_N^- is the ground-state configuration, photons can be absorbed in the $C_N^- \rightarrow C_N^0$ transition, with peak absorption at 4.83 eV, and emission associated with the $C_N^0 \rightarrow C_N^-$ transition is predicted to peak at 3.69 eV. (b) If C_N^0 is the ground-state configuration, photons can be absorbed in the $C_N^0 \rightarrow C_N^+$ transition, with peak absorption at 5.66 eV, and emission associated with the $C_N^+ \rightarrow C_N^0$ transition is predicted to peak at 4.50 eV.

The C_N (0/−) transition level is very similar to those calculated and observed experimentally in Ref. [19]. In that work, it was reported that C_N gives rise to an emission peak at 3.5 eV and an absorption signal peaking at 4.7 eV. These results are within 0.2 eV of our results. In the same study, PL spectra of C-doped AlN showed a broad peak near 3.6 eV for low C concentrations, and absorption measurements showed a broad peak near 4.5–4.8 eV that increased with increasing C concentration. These results also compare reasonably well with our calculated configuration-coordinate diagram in Fig. 6(a). Our results also agree reasonably well with the optical properties of C-doped AlN reported in Ref. [55], in which a 3.9 eV PL signal and a 4.9 eV absorption signal were observed.

In Fig. 6(b) we take C_N^0 as the ground state and consider optical transitions associated with the (+/0) transition level. We find an absorption energy of 5.66 eV, an emission peak at 4.50 eV, and a zero-phonon line of 5.13 eV for these transitions. The additional (+/0) transition for C_N (which was not discussed in Ref. [19]) allows for the possibility that AlN could exhibit a higher-energy luminescence peak for high C doping, or even exhibit a double-peaked PL pattern as we predict for C in GaN. The (+/0) transition may explain why the C-related PL signal shifted to higher energies for higher C concentrations in Ref. [19]. In Ref. [20], a double-peaked PL spectrum was observed in some samples (with peaks near 3.5 and 4.8 eV that are similar to our two predicted C_N transitions), but the possibility of C impurity participation in these samples was not discussed. Broad PL peaks have also been observed near 4.5 eV in other reports [3,21], but disentangling the effects of C and other impurities (such as O and Si) has proven difficult. A broad PL peak near 4.4 eV has been observed in intentionally C-doped AlN [18], but the C concentration in these samples was not reported.

Comparing our results for C_N in AlN and GaN, we observe that the configuration-coordinate diagrams in Fig. 6 are similar to those in Fig. 3: Two emission signals are possible for C_N, and the relaxation energies are similar as well. The most salient difference is the position of the acceptor transition levels with respect to the VBM. This is not surprising, since the carbon acceptor levels are derived from atomiclike C $2p$ states, and the VBM of AlN is known to be lower in energy than that of GaN on an absolute scale [56]. Additional comments on this issue will be made in Sec. III E.

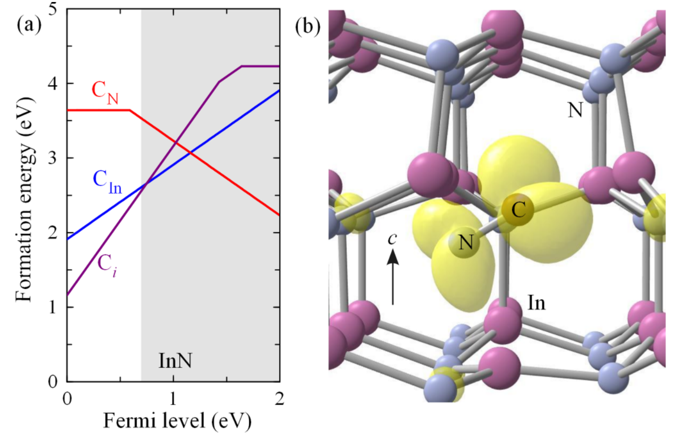

FIG. 7. (Color online) (a) Formation energy versus Fermi level for C_{In}, C_N, and C_i in InN under In-rich conditions. The shaded region indicates Fermi levels above the CBM that may be accessible at sufficiently high electron concentrations (see Ref. [22], and references therein). (b) Local structure of the C_i split interstitial in InN, with yellow lobes indicating the wave function of the π-π states. The isosurface is set to 5% of the maximum.

D. Carbon impurities in InN

1. C_{In} in InN

The calculated formation energies as a function of Fermi-level position for C in InN are shown in Fig. 7. Since the formation enthalpy of InN is small (see Table I), we present only the results for In-rich conditions; under N-rich conditions the formation energies would change by only 0.2 eV. We find that C_{In} is a shallow donor, present only in the 1+ charge state for Fermi levels within the band gap. The high formation energy of C_{In} in InN reflects the large size mismatch between C and In. For C_{In}^+, the C atom moves off the In lattice site by 0.69 Å, and forms a 1.42 Å bond with three N nearest neighbors (these three N atoms also move off their sites, moving towards the C atom by 0.65 Å). The remaining N atom is displaced off its lattice site, and moves away from the C impurity by 5% of the bulk In-N bond length.

2. C_N in InN

As in GaN and AlN, C_N in InN acts a deep acceptor, with the (0/−) transition level located at 0.59 eV above the VBM. The hole associated with C_N^0 is localized on the carbon impurity, as this deep level is related to C $2p$ states. Together with the localization of the hole we again find a distortion whereby the nearest neighbor In atoms are displaced away from C_N by 2% of the bulk bond length. For C_N^-, the C-In bond lengths differ by less than 0.5% from the bulk In-N bond lengths.

Unlike in the other nitrides, we do not find a (+/0) transition level for C_N inside the band gap of InN. We do find a locally stable configuration for C_N^+, but the (+/0) transition level is found at 0.05 eV below the VBM of InN.

3. C_i in InN

A major difference from GaN and AlN occurs for the carbon interstitial C_i which is found to be significantly lower in energy than either C_{In} or C_N in InN. As shown in Fig. 7(a), for Fermi levels ranging from the VBM to the CBM of InN, C_i^{2+} is the lowest-energy configuration of the carbon impurity. The structure of this defect is of the split-interstitial type, as shown in Fig. 7(b). The C atom forms a 1.17 Å bond with a bulk N atom, and causes a strong outward relaxation of the next-nearest In neighbors. The charge distribution of the defect state in the gap is shown in Fig. 7(b), indicating the π-π interaction within the C-N split interstitial. The electronic structure of this defect is very similar to that of the split interstitials found for carbon and nitrogen impurities in ZnO, reported in Ref. [57].

Our results indicate that carbon doping in InN will contribute to n-type conductivity, as long as the Fermi level is less than 1 eV above the VBM. Our calculations also indicate that C_i should be a stable species in InN. Using nudged-elastic band calculations, we find that the migration barrier of C_i is 1.6 eV. Based on an approach described in Ref. [58] and using a prefactor of 10^{13} s^{-1}, representing the phonon frequency, we estimate that C_i in InN will become mobile at 620 K.

The short bond length of the C-N split interstitial in InN leads to characteristic vibrational modes that could be observed experimentally in C-doped InN with vibrational spectroscopy. We find that C_i in InN leads to a vibrational mode of 2270 cm^{-1}, based on stretching of the C-N bond. This is very distinct from bulk InN phonon modes (which occur in the 80–600 cm^{-1} range, Ref. [59]), indicating that this mode should be observable.

Above the CBM of InN, the C_{In}^+ donor is the most stable C-related species, and remains so until E_F is 0.46 eV above the CBM. This indicates that C will continue to act as a donor even at fairly high levels of n-type doping, as has been observed in a recent study [22].

E. Alignment of the transition levels of C_N

Having performed calculations for C_N in AlN, GaN, and InN, it is of interest to examine whether any trends or systematic behavior can be identified. We have found that the charge-state transition levels for C_N in these three materials occur at significantly different energies; however, a systematic trend appears if we plot the results on an absolute energy scale. This can be accomplished by using the band alignments calculated in Ref. [56], as shown in Fig. 8. Comparing the positions of the C_N (0/−) and (+/0) levels in InN, GaN, and AlN, we find that each transition level aligns within 0.2 eV on an absolute scale. We attribute this to the fact that the (0/−) and (+/0) levels of the carbon impurity involve adding and removing an electron to or from defect states that are mainly atomiclike $2p$ orbitals residing in the semiconductor band gap.

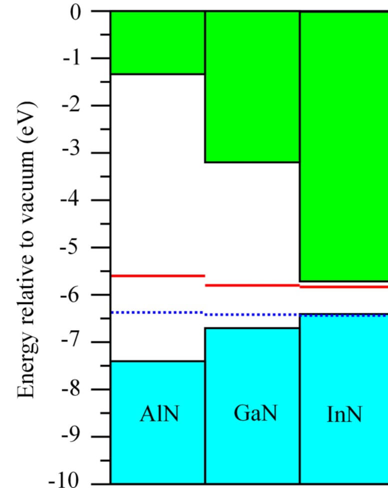

FIG. 8. (Color online) Charge-state transition levels of C_N acceptors in AlN, GaN, and InN, with the band structures aligned on an absolute energy scale [56]. The (0/−) transition levels are indicated by solid lines and the (+/0) transition levels are indicated by dotted lines.

IV. CONCLUSIONS

Using hybrid density functional calculations we have investigated the electrical and optical properties of carbon impurities in GaN, AlN, and InN. In contrast to results based on local or semilocal functionals, we find that C_N is a deep acceptor in all nitrides studied here and exhibits AX behavior. C_N is the lowest-energy configuration of the carbon impurity under n-type conditions in GaN and AlN, and in both materials the carbon acceptor can give rise to two distinct PL signals. We find shallow-donor behavior for C_{Ga} in GaN and C_{In} in InN, but in AlN C_{Al} acts as a DX center. In InN, C_i is the most stable site for the carbon impurity across the semiconductor band gap, where it acts as a donor and can contribute to n-type conductivity.

ACKNOWLEDGMENTS

We thank D. Steiauf, J. Speck, S. Ringel, and S. Keller for useful discussions. The work was supported by NSF (Grant No. DMR-0906805), by the UCSB Solid State Lighting and Energy Center, and by the Center for Low Energy Systems Technology (LEAST), one of the six SRC STARnet Centers, sponsored by MARCO and DARPA. Computational resources were provided by the Center for Scientific Computing at the CNSI and MRL (an NSF MRSEC, Grant No. DMR-1121053) (Grant No. NSF CNS-0960316), and by the Extreme Science and Engineering Discovery Environment (XSEDE), supported by NSF (Grant No. OCI-1053575 and NSF Grant No. DMR07-0072N).

[1] S. Nakamura, T. Mukai, and M. Senoh, Appl. Phys. Lett. **64**, 1687 (1994).
[2] U. K. Mishra, P. Parikh, and Y. F. Wu, Proc. IEEE **90**, 1022 (2002).
[3] M. Strassburg, J. Senawiratne, N. Dietz, U. Haboeck, A. Hoffmann, V. Noveski, R. Dalmau, R. Schlesser, and Z. Sitar, J. Appl. Phys. **96**, 5870 (2004).

[4] St. Keller, P. Cantu, C. Moe, Y. Wu, Sa. Keller, U. K. Mishra, J. S. Speck, and S. P. DenBaars, Jpn. J. Appl. Phys. **44**, 7227 (2005).
[5] H. Timmers, K. S. A. Butcher, S. K. Shrestha, P. P.-T. Chen, M. Wintrebert-Fouquet, and R. Dogra, J. Cryst. Growth **288**, 236 (2006).
[6] C. Poblenz, P. Waltereit, S. Rajan, S. Heikman, U. K. Mishra, and J. S. Speck, J. Vac. Sci. Technol. B **22**, 1145 (2004).
[7] A. Armstrong, A. R. Arehart, B. Moran, S. P. DenBaars, U. K. Mishra, J. S. Speck, and S. A. Ringel, Appl. Phys. Lett. **84**, 374 (2004).
[8] S. W. Kaun, P. G. Burke, M. H. Wong, E. C. H. Kyle, U. K. Mishra, and J. S. Speck, Appl. Phys. Lett. **101**, 262102 (2012).
[9] A. F. Wright, J. Appl. Phys. **92**, 2575 (2002).
[10] J. L. Lyons, A. Janotti, and C. G. Van de Walle, Appl. Phys. Lett. **97**, 152108 (2010).
[11] E. E. Reuter, R. Zhang, T. F. Kuech, and S. G. Bishop, MRS Internet J. Nitride Semicond. Res. **4S1**, G3.67 (1999).
[12] T. Ogino and M. Aoki, Jpn. J. Appl. Phys. **19**, 2395 (1980).
[13] C. H. Seager, A. F. Wright, J. Yu, and W. Götz, J. Appl. Phys. **92**, 6553 (2002).
[14] B. K. Meyer, *Semiconductors and Semimetals* (Academic, New York, 1999), Vol. 57, pp. 371–406.
[15] D. S. Green, U. K. Mishra, and J. S. Speck, J. Appl. Phys. **95**, 8456 (2004).
[16] R. Armitage, Q. Yang, and E. R. Weber, J. Appl. Phys. **97**, 073524 (2005).
[17] C. H. Seager, D. R. Tallant, J. Yu, and W. Götz, J. Lumin. **106**, 115 (2004).
[18] X. Tang, F. Hossain, K. Wongchotigul, and M. G. Spencer, Appl. Phys. Lett. **72**, 1501 (1998).
[19] R. Collazo, J. Xie, B. E. Gaddy, Z. Bryan, R. Kirste, M. Hoffmann, R. Dalmau, B. Moody, Y. Kumagai, T. Nagashima, Y. Kubota, T. Kinoshita, A. Koukitu, D. L. Irving, and Z. Sitar, Appl. Phys. Lett. **100**, 191914 (2012).
[20] B. Bastek, F. Bertram, J. Christen, T. Hempel, A. Dadgar, and A. Krost, Appl. Phys. Lett. **95**, 032106 (2009).
[21] G. A. Slack, L. J. Schowalter, D. Morelli, and J. A. Freitas, Jr., J. Cryst. Growth **246**, 287 (2002).
[22] M. Himmerlich, A. Knübel, R. Aidam, L. Kirste, A. Eisenhardt, S. Krischok, J. Pezoldt, P. Schley, E. Sakalauskas, R. Goldhan, R. Félix, J. M. Mánuel, F. M. Morales, D. Carvalho, T. Ben, R. García, and G. Koblmüller, J. Appl. Phys. **113**, 033501 (2013).
[23] L. E. Ramos, J. Furthmüller, J. R. Leite, L. M. R. Scolfaro, and F. Bechstedt, Phys. Status Solidi B **234**, 864 (2002).
[24] T. A. G. Eberlein, R. Jones, S. Öberg, and P. R. Briddon, Appl. Phys. Lett. **91**, 132105 (2007).
[25] X. M. Duan and C. Stampfl, Phys. Rev. B **79**, 035207 (2009).
[26] P. Bogusławski and J. Bernholc, Phys. Rev. B **56**, 9496 (1997).
[27] A. Fara, F. Bernardini, and V. Fiorentini, J. Appl. Phys. **85**, 2001 (1999).
[28] J. L. Lyons, A. Janotti, and C. G. Van de Walle, Phys. Rev. B **80**, 205113 (2009).
[29] J. L. Lyons, A. Janotti and C. G. Van de Walle, Appl. Phys. Lett. **95**, 252105 (2009).
[30] A. Janotti, C. Franchini, J. B. Varley, G. Kresse, and C. G. Van de Walle, Phys. Status Solidi RRL **7**, 199 (2013).
[31] J. B. Varley, J. R. Weber, A. Janotti, and C. G. Van de Walle, Appl. Phys. Lett. **97**, 142106 (2010).
[32] A. Alkauskas, P. Broqvist, and A. Pasquarello, Phys. Status Solidi B **248**, 775 (2011).
[33] Á. Szabó, N. T. Son, E. Janzén, and A. Gali, Appl. Phys. Lett. **96**, 192110 (2010).
[34] D. J. Chadi and K. J. Chang, Phys. Rev. Lett. **61**, 873 (1988).
[35] D. J. Chadi, Appl. Phys. Lett. **59**, 3589 (1991).
[36] W. Kohn and L. J. Sham, Phys. Rev. **140**, A1133 (1965).
[37] J. Heyd, G. E. Scuseria, and M. Ernzerhof, J. Chem. Phys. **118**, 8207 (2003).
[38] G. Kresse and J. Furthmüller, Phys. Rev. B. **54**, 11169 (1996).
[39] G. Kresse and J. Furthmüller, Comput. Mater. Sci. **6**, 15 (1996).
[40] J. P. Perdew, K. Burke, and M. Ernzerhof, Phys. Rev. Lett. **77**, 3865 (1996).
[41] *Semiconductors–Basic Data*, 2nd revised ed., edited by O. Madelung (Springer, Berlin, 1996).
[42] P. E. Blöchl, Phys. Rev. B **50**, 17953 (1994).
[43] G. Kresse and D. Joubert, Phys. Rev. B **59**, 1758 (1999).
[44] C. G. Van de Walle and J. Neugebauer, J. Appl. Phys. **95**, 3851 (2004).
[45] C. Freysoldt, J. Neugebauer, and C. G. Van de Walle, Phys. Rev. Lett. **102**, 016402 (2009).
[46] C. Freysoldt, J. Neugebauer, and C. G. Van de Walle, Phys. Status Solidi B **248**, 1067 (2011).
[47] A. Alkauskas, J. L. Lyons, D. Steiauf, and C. G. Van de Walle, Phys. Rev. Lett. **109**, 267401 (2012).
[48] G. Meneghesso, F. Rossi, G. Salviati, M. J. Uren, E. Muñoz, and E. Zanoni, Appl. Phys. Lett. **96**, 263512 (2010).
[49] P. B. Klein, S. C. Binari, K. Ikossi, A. E. Wickenden, D. D. Koleske, and R. L. Henry, Appl. Phys. Lett. **79**, 3527 (2001).
[50] P. B. Shah, R. H. Dedhia, R. P. Tompkins, E. A. Viveiros, and K. A. Jones, Solid-State Electron. **78**, 121 (2012).
[51] A. Armstrong, A. R. Arehart, D. Green, U. K. Mishra, J. S. Speck, and S. A. Ringel, J. Appl. Phys. **98**, 053704 (2005).
[52] U. Honda, Y. Yamada, Y. Tokuda, and K. Shiojima, Jpn. J. Appl. Phys. **51**, 04DF04 (2012).
[53] D. O. Demchenko, I. C. Diallo, and M. A. Reshchikov, Phys. Rev. Lett. **110**, 087404 (2013).
[54] J. Neugebauer and C. G. Van de Walle, Appl. Phys. Lett. **68**, 1829 (1996).
[55] T. Nagashima, Y. Kubota, T. Kinoshita, Y. Kumagai, J. Xie, R. Collazo, H. Murakami, H. Okamoto, A. Koukitu, and Z. Sitar, Appl. Phys. Exp. **5**, 125501 (2012).
[56] C. G. Van de Walle and J. Neugebauer, Nature (London) **423**, 626 (2003).
[57] S. Limpijumnong, X. Li, S. H. Wei, and S. B. Zhang, Appl. Phys. Lett. **86**, 211910 (2005).
[58] A. Janotti and C. G. Van de Walle, Phys. Rev. B **76**, 165202 (2007).
[59] V. Y. Davydov, V. V. Emtsev, I. N. Goncharuk, A. N. Smirnov, V. D. Petrikov, V. V. Mamutin, V. A. Vekshin, S. V. Ivanov, M. B. Smirnov, and T. Inushima, Appl. Phys. Lett. **75**, 3297 (1999).